Chapter II: Reprogramming Directional Cell Motility by Tuning Micropattern Features and Cellular Signals

1. Abstract

Mammalian cells exhibit directed cell movement on micropatterned surfaces.[1-3] A key challenge is to better understand the parameters and mechanisms that orient cell movement on micropatterns and to apply these insights to modulate rationally cellular traffic on synthetic materials. Here, using quantitative insights gleaned from the analysis of cell movement on teardrop-shaped micropatterns, we re-design the geometrical features of micropatterns to enhance the directional bias and to modulate the flux of cell movement. Furthermore, we demonstrate that perturbing an intracellular signal involved in lamellipodial extensions (Rac1) flips the preferred direction of cell movement. Our findings reveal a key role for lamellipodial extensions in determining the directional bias of cell movement on micropatterns and offer design strategies to modulate and reprogram this bias by manipulating pattern features and cellular signals. These insights begin to lay a foundation for constructing materials for channeling cellular traffic in applications, such as tissue engineering.

Reprinted from K. Kushiro and A.R. Asthagiri from *Advanced Materials* (2010).

2. Introduction

Micropatterned surfaces have been used effectively to control cell shape, survival, proliferation and differentiation.[4-6] More recently, it has been shown that cells can exhibit persistent, directional movement on micropatterned surfaces.[2,3] When cells were released from confinement within a teardrop-shaped micropattern, their initial trajectory favored the blunt end over the tip end.[1] This short-lived bias is consistent with the stereotypical teardrop-like shape ascribed to a migrating cell with a broad leading edge and a narrow trailing tail.[7,8] A more persistent bias in cell movement was observed on a micropattern composed of four disjointed teardrop-shaped islands that are arranged to form a square.[2] On this pattern, the asymmetry of the teardrop defined a major axis for the cell body, but the direction of movement did not favor the blunt or tip end. The direction was dictated by the availability of an adjacent island along the cell body axis.

3. Results

3.1. Key pattern features are necessary for directional cell motility

In this work, we sought to better understand the micropattern features and cellular signals that orient cell movement on micropatterns and to apply these insights to rationally modulate and re-program the directional bias of cell movement. To begin our study, we used the teardrop-shaped micropatterns described previously[2] and quantified the movement tendencies of MCF-10A mammary epithelial cells. The percentage of complete jumps that were made in either direction of the pattern was measured (**Fig. 1**, labeled arrows). Teardrop islands in Pattern A (**Fig. 1A** and **Movie 1**) induced a strong

directional bias in which 81% of the jumps were observed to be sideways from the tip of a teardrop to the blunt end of an adjacent teardrop (sT>B jump), while the remaining 19% of the jumps were head-on from the blunt end of a teardrop to tip of an adjacent teardrop (hB>T jump). Even slight alteration of island placement to Pattern B (**Fig. 1B** and **Movie 2**) eliminated this bias. On Pattern B, 60% of the jumps were observed to be sideways from the blunt end of a teardrop to the tip of an adjacent teardrop (sB>T jump), while the remaining 40% of the jumps were head-on from the tip of a teardrop to the blunt end of an adjacent teardrop (hT>B jump). Patterns lacking asymmetric islands (**Fig. 1C**), gap size (**Fig. 1D, E**) or both (**Fig. 1F**) also exhibited no bias. Thus, only Pattern A exhibited strong directional bias, demonstrating that gap size, teardrop asymmetry and the relative positioning of the teardrops are all essential features.

We have observed the same directional bias in normal human epidermal keratinocytes (NHEK) migrating on similar patterns (**Fig. S1**). It is noteworthy that the directional bias observed here differs from that reported in the previous study involving 3T3 fibroblast and human microvascular endothelial cell (HMVEC) movement on teardrop micropatterns.[2] This difference may be attributed to disparate cell migration properties of mesenchymal versus epithelial cell types (**Fig. S2**) and the significantly different environmental signals, including growth factors and extracellular matrix (ECM) proteins, to which cells were exposed. That different cell types exhibit distinct movement tendencies is expected and has been documented, for example, in tumor cells with different requirements for extracellular proteolysis.[9] The key question of interest here is whether and how the movement bias can be rationally re-programmed by modulating micropattern features and key cellular signals.

3.2. Geometrical modification based on quantitative jump analysis enhances directional bias

Based on our quantitative measurements of cell movement on teardrop squares, we sought to design a new pattern that enhances the directional bias. The preference for sT>B jumps on Pattern A (Fig. 1A) was only 80% with the other 20% involving hB>T jumps. We reasoned that the bias for sT>B jump may be further enhanced if this jump option were juxtaposed against an even more unfavorable type of jump. One possibility for a highly unfavorable jump came from the observations of cell movement on Pattern B (Fig. 1B). Cell movement on Pattern B was not only unbiased, but also the frequency of jumps was significantly lower than on Pattern A (**Table S1**). These observations suggested that the hB>T and sT>B jumps are highly unfavorable and could be ideal candidates to juxtapose against the highly favored sT>B jump from Pattern A.

Thus, we designed a new yin-yang pattern that juxtaposed the sB>T jump against the sT>B jump and where only sideway jumps are possible (sB>T or sT>B jumps; **Fig. 1G**). As a control, we designed another yin-yang pattern where only head-on jumps are possible (**Fig. 1H**) at both ends of the curved teardrop. Consistent with our hypothesis, the sideways yin-yang pattern resulted in an enhanced T>B directional bias (91%; **Movie 3**) compared to the original Pattern A in which the T>B directional bias was 80%. In contrast, the control head-on yin-yang pattern yielded little bias in cell movement.

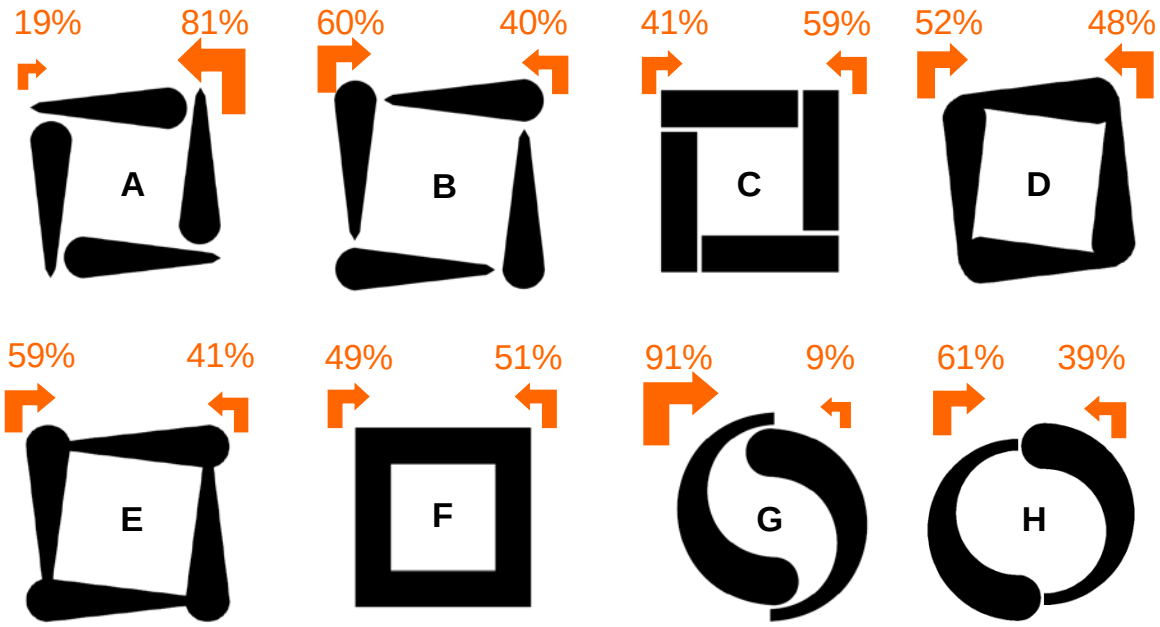

Figure 1. Directional bias of MCF-10A epithelial cells on teardrop-based micropatterns. Standard dimensions for the adhesive islands were 20 μm in width and 80μm in length with 3μm non-adhesive gaps between islands. The width of the teardrop is 3 μm at the tip and 20 μm at the blunt end. The patterns are: (**A**) disjointed teardrops with the blunt end running into a tip, (**B**) disjointed teardrops with tip running into the blunt end, (**C**) disjointed adhesive islands lacking asymmetry, (**D**) Pattern A without gaps, (**E**) Pattern B without gaps, (**F**) pattern with both gaps and island asymmetry eliminated, (**G**) sideways yin-yang pattern and (**H**) head-on yin-yang pattern. Percentages of complete jumps in each direction are shown (greater than 100 jumps quantified for each pattern).

3.3. Signal alteration based on lamellipodial observations flips directional bias

In addition to using quantitative analysis of movement tendencies to engineer patterns with enhanced directional bias, we sought to better understand the preference that epithelial cells exhibit for the sT>B jump as opposed to the sB>T jump or the head-on alternatives. We examined more closely the sT>B jump at 63x magnification. On Pattern A, we noticed that as the lamellipodium of a moving cell becomes constrained at the tip end of a teardrop, the cell extends a new side lamellipodium that is stabilized by latching onto a lateral island (**Fig. 2A** and **Movie 4**). In sharp contrast, Pattern B does not provide a lateral island to stabilize a new side lamellipodia; thus, in order to jump onto an adjacent island, cells encountering a tip on Pattern B must use their pre-existing spatially-constrained lamellipodia to reach out in a headlong direction (**Movie 5**). Thus, high directional bias seems to be the consequence of side lamellipodial protrusions at the tip ends that are stabilized by adhesions to a lateral, adjacent island.

This observation of side lamellipodium formation suggested that the bias of the cells on these micropatterns may be sensitive to intracellular signals that control lamellipodial extensions, such as Rac1, a small GTPase signaling protein. Specifically, moderate Rac1 knockdown has been shown to reduce the formation of new lamellipodia and increase the directional persistence of cells on non-patterned tissue culture substrates.[10] Thus, we reasoned that moderate Rac1 suppression may enhance the stability of a pre-existing lamellipodium and thereby improve the ability to make head-on jumps instead of switching direction via a sideways jump.

To test this hypothesis, we suppressed the expression level of Rac1 by ~60% using RNA interference (**Fig. S3**). MCF-10A cells with reduced Rac1 expression exhibited a different motility bias compared to cells transfected with control siRNA (**Fig. 2B**). Rac1 suppression significantly reduced the bias for sT>B jumps in Pattern A (90% to 61%; Fig. 2B and **Movie 6**) and increased the bias for hT>B jumps in Pattern B (53% to 80%; Fig. 2B and **Movie 7**). By discouraging sideways jumps and promoting head-on jumps, we dampened the biased movement on Pattern A and created a new bias on the previously ineffective Pattern B. Conferring this new bias in movement comes with an expected cost in the speed of cell movement: due to dampened lamellipodial activity in cells transfected with Rac1 RNAi, the speed of migration and frequency of jumps were reduced. These results demonstrate that the directional bias of cell motility on micropatterned surfaces may be re-programmed by tuning an intracellular signal that regulates lamellipodial extensions.

It is noteworthy that attenuating Rac1 expression enhances the tendency of cells to hop in a direction parallel to the major axis of the teardrop. On Pattern B, the preference for hops parallel to the teardrop axis (hT>B jump) increases from 53% (control siRNA) to 80% (Rac1 siRNA). The result is a movement bias that closely resembles that reported previously for fibroblasts and HMVEC on similar patterns.[2] On Pattern A, Rac1 suppression has a similar effect although the conversion is not complete: the preference to hop parallel to the major axis of the teardrop (hB>T jump) increases from 10% (control siRNA) to 39% (Rac1 siRNA). These results are consistent with our hypothesis that partial suppression of Rac1 stabilizes pre-existing lamellipodia, thereby enhancing the ability to make headlong jumps. It also suggests that Rac1 level may be a

molecular determinant of the observed differences in the movement preference of fibroblasts/HMVEC versus epithelial cells and may serve as a quantitative index to predict the movement of other cell lines on micropatterns

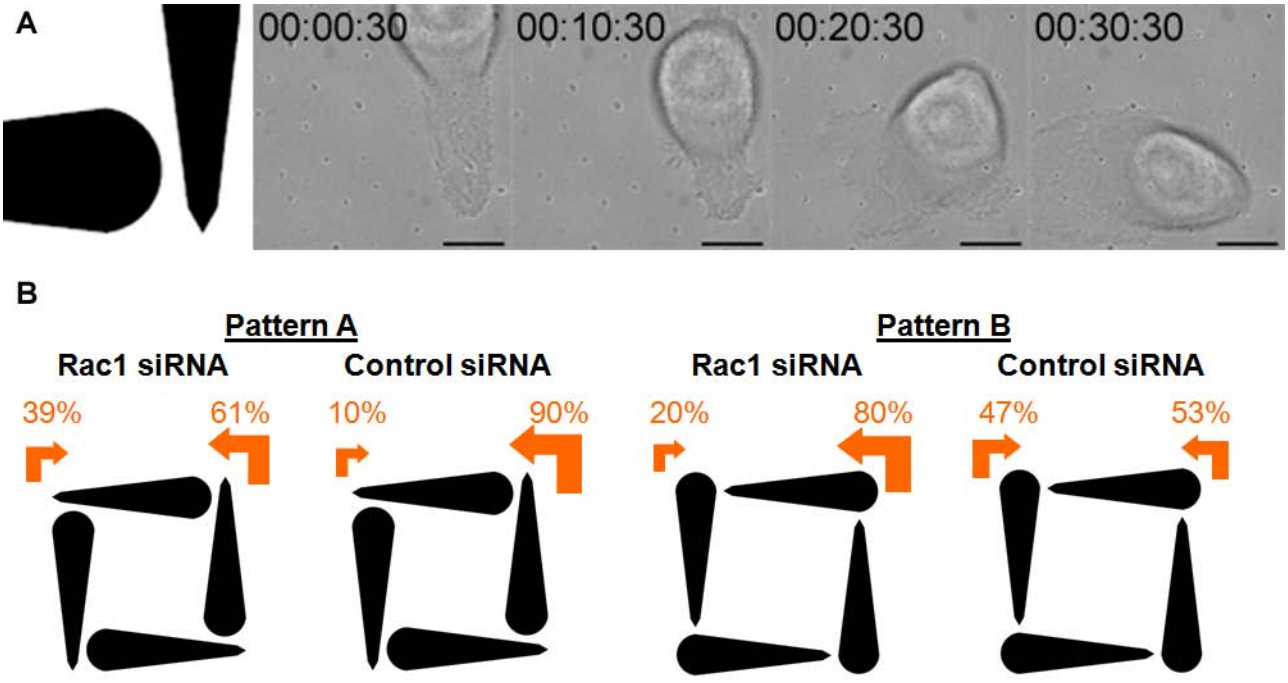

Figure 2. The role of lamellipodial extensions in determining the directional bias of cell movement on micropatterns. (**A**) Timelapse images show the formation of a new, side lamellipodium as a cell jumps sideways from the tip to a blunt end on Pattern A. The corner of Pattern A at which the cell is jumping is shown in the first panel. The time stamps correspond to Movie 4, displayed in h:min:s. (**B**) The effect of Rac1 knockdown on the directional bias of MCF-10A cells on micropatterned surfaces. Directional bias of Rac1 siRNA-treated and control siRNA-treated cells on Pattern A and Pattern B are

shown. Percentages of complete jumps in each direction are shown (greater than 100 jumps quantified for each pattern).

3.4. Novel splitter design modulates cell flux

In addition to re-programming the directional bias, it is desirable to tune the flux of cell movement on synthetic materials. To explore this possibility, we adapted the aforementioned teardrop micropatterns into a "splitter" design (**Fig. 3A**). Cells originating in the source island (S) would jump to one of the available lateral target islands (T1 and T2). We reasoned that by varying the position of T2, the relative flux of cells moving to T1 versus T2 may be modulated. Thus, we designed micropatterns with the relative position of S and T1 fixed while varying the gap distance or the position offset of T2.

These splitter features have qualitatively distinct effects. Cell movement is highly sensitive to gap distance, displaying a switch-like transition as the gap distance is shifted from 3 to 5 μm (**Fig. 3B**). On the other hand, position offset provided a graded transition as the offset is increased from 0 to 15μm (**Fig. 3C**). Cells had a higher likelihood of jumping to T1 with no offset, and this bias can be gradually increased to near 100% by increasing the offset of T2. These results suggest that varying the offset can be useful in modulating the relative flux of cells along two micropatterned lanes emanating from a splitter design.

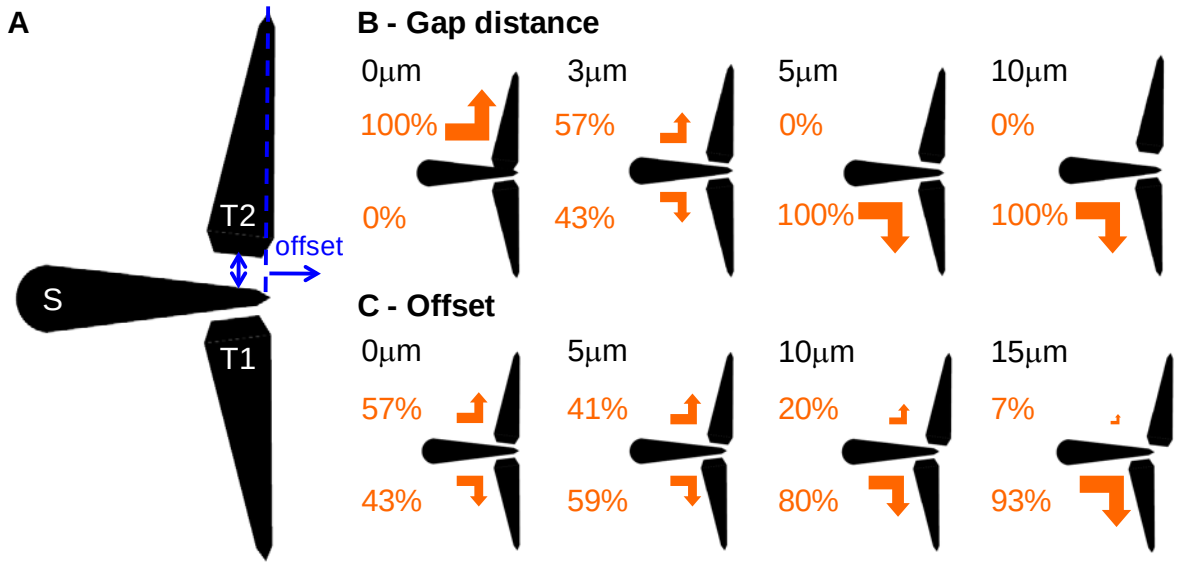

Figure 3. The effect of splitter design features on the directional bias. (**A**) Cells jumping from the source island (S) to adjacent target islands (T1 or T2) were counted. While the positions of S and T1 were held fixed, (**B**) the gap distance and (**C**) the position offset of T2 were varied. Percentages of complete jumps in each direction are shown (greater than 100 jumps were quantified for each pattern).

4. Conclusion

An emerging property of micropatterned surfaces is their ability to orient cell movement.[1-3] Our signal perturbation experiments along with quantitative analysis of cell movement tendencies reveal a key role for lamellipodial extensions and stabilization in determining the directional bias of epithelial cells on micropatterned surfaces. Manipulating pattern features and cellular signals to exploit and modulate lamellipodial

extensions enables both quantitative tuning and qualitative re-programming of the directional bias of cell movement. These findings provide a foundation for modulating the direction and flux of epithelial cell movement on micropatterned surfaces as a powerful complement to gradient-based approaches.[11-13] Together with similar studies focused on other cell types, we envision developing a complete toolbox for programming cellular traffic on micropatterned surfaces for applications, such as tissue engineering.

5. Experimental Methods

5.1. Fabrication of micropatterned substrates

Microcontact printing with a polydimethylsiloxane (PDMS) stamp was used to pattern the adhesion ligand, fibronectin, onto a gold-coated coverslide. Briefly, the PDMS stamp is micro-fabricated using the standard photolithographic techniques [14]; UV light is passed through a chrome mask containing the pattern (Nanoelectronics Research Facility, UCLA) onto a layer of SU-8 photoresist to make a mold, onto which PDMS is cast to make the stamp. The stamp is then "inked" with 16-Mercaptohexadecanoic acid (Sigma Aldrich) dissolved in 99% ethanol and used to print the pattern onto a gold-coated chambered coverslide (Labtek). The unprinted area is passivated using PEG(6)-Thiol (Prochimia) dissolved in 99% ethanol to prevent non-specific binding of cells. After washing with PBS twice, EDC and Sulfo-NHS (Pierce) dissolved in PBS is added to the coverslide to activate the acid to crosslink covalently with the amine group of the subsequently added fibronectin (Sigma Aldrich) dissolved in PBS at 10μg/mL. Finally, BSA conjugated with Alexa Fluor 594 (Invitrogen) was doped into the fibronectin solution for the purpose of pattern visualization (**Fig. S4**).

5.2. Cell culture

MCF-10A human epithelial cells were cultured in growth medium composed of Dulbecco's modified Eagle's medium/Ham's F-12 containing HEPES and L-glutamine (DMEM/F12, Invitrogen) supplemented with 5% horse serum (Invitrogen), 1% penicillin/streptomycin, 10 µg/mL insulin (Sigma), 0.5 µg/mL hydrocortizone (Sigma), 20ng/mL EGF (Peprotech) and 0.1 µg/mL cholera toxin (Sigma) and maintained under humidified conditions at 37ºC and 5% CO_2. Cells were passaged regularly by dissociating confluent monolayers with 0.05% trypsin-EDTA (Invitrogen) and suspending cells in DMEM/F12 supplemented with 20% horse serum and 1% penicillin/streptomycin. After two washes, cells were diluted 1:4 and plated in growth medium.

5.3. Time-lapse microscopy

Cells were seeded in growth medium for 1 hr onto the micropatterned substrate. After washing to remove non-adherent cells, the culture was incubated with fresh growth medium for 1 hr and imaged at 10x magnification every 5 min for 12 hr or at 63x magnification every 30 sec for 2 hr. For siRNA-treated cells, the seeding time was increased by 2 hours. Cells were maintained at 37ºC and 5% CO_2 in a heated chamber with temperature and CO_2 controller (Pecon) during time-lapse imaging. Images and movies were acquired using Axiovert 200M microscope (Carl Zeiss), and Axio Vision LE Rel. 4.7 (Carl Zeiss) was used for image analysis.

5.4. siRNA knockdown

siRNA targeting human Rac1 mRNAs (siGENOME SMARTpool, M-003560-06-0005) and non-targeting siRNA (siGENOME Non-Targeting siRNA pool #2, D-001206-14-05) were obtained from Thermo Scientific. Cells were transfected with 20 nM siRNA using lipofectamine RNAiMAX 2000 (Invitrogen).

6. Acknowledgements

We thank the members of the Asthagiri group for helpful discussions. This research was funded by the NSF Center for Science and Engineering of Materials at Caltech. We also gratefully acknowledge the technical support and infrastructure provided by the Kavli Nanoscience Institute. Supporting Information is available online from Wiley InterScience or from the author.

7. References

[1] X. Jiang, D. A. Bruzewicz, A. P. Wong, M. Piel, G. M. Whitesides, *Proc Natl Acad Sci U S A* **2005**, *102*, 975.

[2] G. Kumar, C. C. Ho, C. C. Co, *Advanced Materials* **2007**, *19*, 1084.

[3] G. Mahmud, C. J. Campbell, K. J. M. Bishop, Y. A. Komarova, O. Chaga, S. Soh, S. Huda, K. Kandere-Grzybowska, B. A. Grzybowski, *Nature Physics* **2009**, *5*, 606.

[4] C. S. Chen, M. Mrksich, S. Huang, G. M. Whitesides, D. E. Ingber, *Science* **1997**, *276*, 1425.

[5] R. McBeath, D. M. Pirone, C. M. Nelson, K. Bhadriraju, C. S. Chen, *Developmental Cell* **2004**, *6*, 483.

[6] R. Singhvi, A. Kumar, G. P. Lopez, G. N. Stephanopoulos, D. I. C. Wang, G. M. Whitesides, D. E. Ingber, *Science* **1994**, *264*, 696.

[7] D. A. Lauffenburger, A. F. Horwitz, *Cell* **1996**, *84*, 359.

[8] A. J. Ridley, M. A. Schwartz, K. Burridge, R. A. Firtel, M. H. Ginsberg, G. Borisy, J. T. Parsons, A. R. Horwitz, *Science* **2003**, *302*, 1704.

[9] K. Wolf, I. Mazo, H. Leung, K. Engelke, U. H. von Andrian, E. I. Deryugina, A. Y. Strongin, E. B. Brocker, P. Friedl, *Journal of Cell Biology* **2003**, *160*, 267.

[10] R. Pankov, Y. Endo, S. Even-Ram, M. Araki, K. Clark, E. Cukierman, K. Matsumoto, K. M. Yamada, *Journal of Cell Biology* **2005**, *170*, 793.

[11] S. B. Carter, *Nature* **1965**, *208*, 1183.

[12] C. M. Lo, H. B. Wang, M. Dembo, Y. L. Wang, *Biophys J* **2000**, *79*, 144.

[13] J. Y. Wong, A. Velasco, P. Rajagopalan, Q. Pham, *Langmuir* **2003**, *19*, 1908.

[14] S. Raghavan, C. S. Chen, *Advanced Materials* **2004**, *16*, 1303.

8. Supporting Information

8.1. Supporting figures

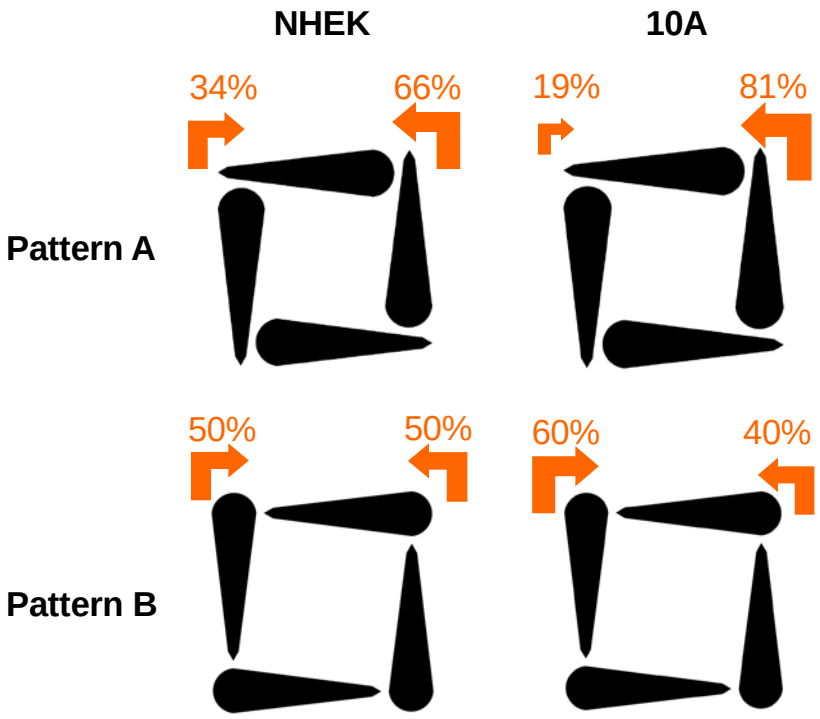

Figure S1. Directional bias of normal human epidermal keratinocytes (NHEK) on Patterns A and B. The directional bias for MCF-10A epithelial cells (right column) is also displayed.

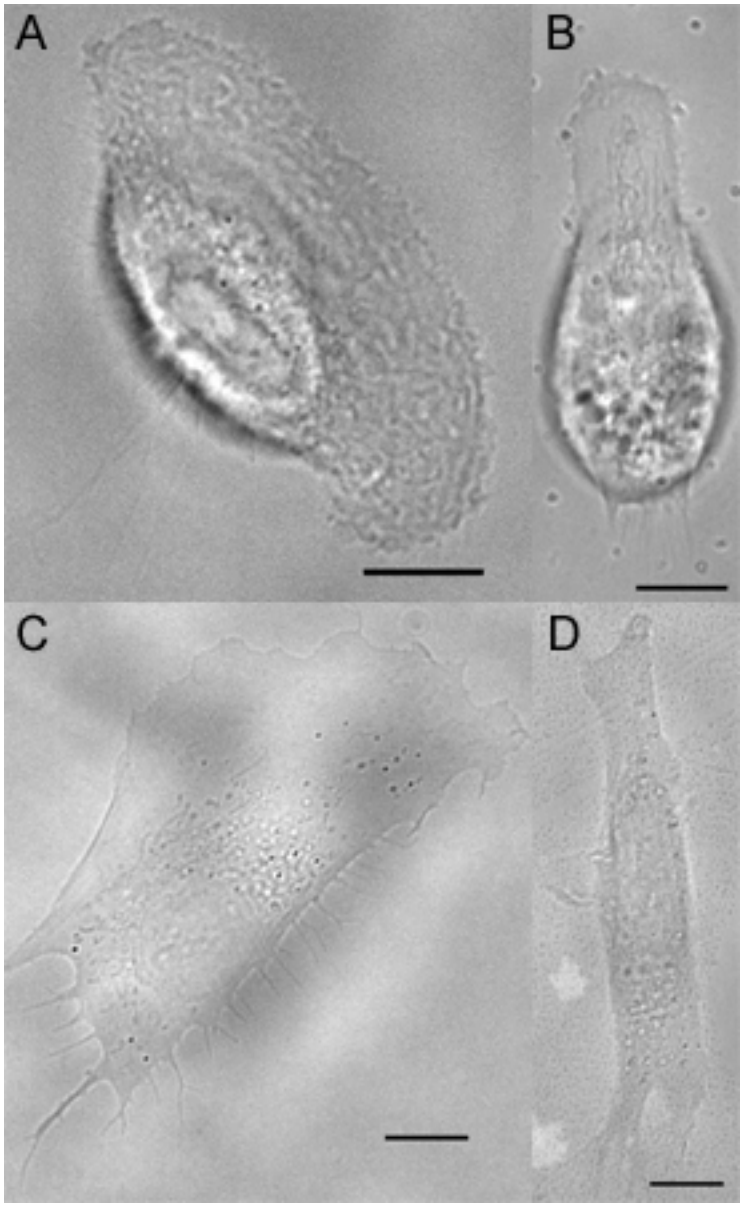

Figure S2. Morphology of migrating MCF-10A epithelial cells and Rat1 fibroblasts. MCF-10A cells on (**A**) uniform, non-patterned surface exhibit a clear, broad lamellipodium, while cells on (**B**) 10μm line pattern exhibit a highly motile morphology with a lamellipodium constrained by the width of the micropattern. In sharp contrast, Rat1 fibroblasts on (**C**) uniform, non-patterned surface exhibit multiple lamellipodia,

while fibroblasts on (**D**) 10μm line pattern exhibit a less motile morphology with active lamellipodia on two ends despite the constraints by the width of the micropattern. Scale bar, 10μm.

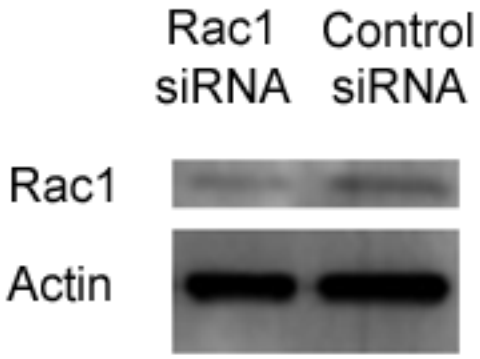

Figure S3. Effect of RNA interference on Rac1 expression level. Western blot image of Rac1 siRNA knockdown. Concentration of siRNA was 20nM and Rac1 expression level was reduced to 40% of the control, as quantified by Versadoc Imaging System.

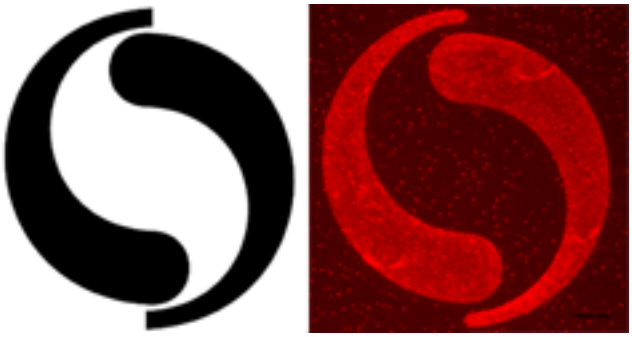

Figure S4. Fluorescence imaging of the underlying micropattern via BSA-Cy3. Scale bar, 10μm.

8.2. Supporting table

Table S1. Detailed analysis of the jumps of MCF-10A epithelial cells from either blunt or tip ends over two experiments. Note that cells on pattern B jump less successfully.

	Blunt End			**Tip End**		
	Successful Attempts [a]	Unsuccessful Attempts [b]	No Visible Attempts [c]	Successful Attempts	Unsuccessful Attempts	No Visible Attempts
Pattern A	31	13	66	165	24	61
Pattern B	13	9	25	9	6	29

[a] Successful attempt corresponds to a complete translocation of cells from one island to the other. [b] Unsuccessful attempt corresponds to a failed lamellipodial extension to an adjacent island which subsequently retracts. [c] No visible attempt corresponds to a reversal of movement direction without any attempt to jump to an adjacent island.

8.3. Movie legends

Movie 1. MCF-10A cell migrating with high bias on Pattern A. This pattern is depicted in Fig. 1A and in the first frame of this movie. Images were acquired every 5 min for 8.6 h (103 frames) and compiled at 10 frames/s in the movie. Scale bar, 20μm.

Movie 2. MCF-10A cell migrating with low bias on Pattern B. This pattern is depicted in Fig. 1B and in the first frame of this movie. Images were acquired every 5 min for 12 h (144 frames) and compiled at 10 frames/s in the movie. Scale bar, 20μm.

Movie 3. MCF-10A cells migrating with high bias on sideways yin-yang pattern. This pattern is depicted in Fig. 1G and in the first frame of this movie. This movie shows two cells moving on two separate yin-yang patterns (top and bottom). Images were acquired every 5 min for 12 h (144 frames) and compiled at 10 frames/s in the movie. Scale bar, 20μm.

Movie 4. Formation of new, side lamellipodia when jumping from the tip to a blunt end on Pattern A (63x magnification). Images were acquired every 30 s for 0.7 h (81 frames) and compiled at 10 frames/s in the movie. The first frame shows the region of the micropattern on which the cell is moving. Scale bar, 10μm.

Movie 5. Lack of new, side lamellipodia when jumping from tip end on Pattern B (63x magnification). Images were acquired every 30 s for 0.8 h (101 frames) and compiled at 10 frames/s in the movie. The first frame shows the region of the micropattern on which the cell is moving. Scale bar, 10μm.

Movie 6. Rac1 siRNA-treated MCF-10A cell with reduced bias on Pattern A. This pattern is depicted in Fig. 1A and in the first frame of this movie. Images were acquired every 5 min for 12 h (144 frames) and compiled at 10 frames/s in the movie. Scale bar, 20μm.

Movie 7. Rac1 siRNA-treated MCF-10A cell with increased bias on Pattern B. This pattern is depicted in Fig. 1B and in the first frame of this movie. Images were acquired every 5 min for 10.8 h (130 frames) and compiled at 10 frames/s in the movie. Scale bar, 20μm.